Universitat Politècnica de Catalunya

Escola Tècnica Superior d'Enginyeria Industrial de Barcelona. ETSEIB

Design, modeling and simulation of a PV power plant.

Bachelor's final project

Autor: Pablo Poza Ferragut

Supervisor: Oriol Gomis Bellmunt

Junio 2020

Summary

The rise of the photovoltaic energy during the last decades and mainly during the last years has many indicators; the fast growth of the global production capacity, the innovations related to the solar energy technologies or the continuous adaptation of the law code to fit a wider variety of scenarios and conditions.

Additionally the recent improvements have given Large Scale PV power plant (LS-PVPP) the capability to work as baseload power plants relieving dirtier sources of energies. However one of the biggest disadvantages in front of conventional energy sources is the cost. In the last years PV technologies have achieved higher cost-effective ratio and now are able to compete against non-renewable production methods.

For this reason the present work is centered in the development of a tool for integration of LS-PVPP in the actual energy distribution system that allows the user to optimize and study the design and functionality of the plant.

A MATLAB based program and different functions have been developed to perform a power flow analysis. Different grid codes requirements have been analyzed for LS-PVPP. Approaches from different years are taken into account and the tendency of unifying some parts of these grid codes to achieve higher levels of energy share is discussed too. Examples of control implementation to meet these requirements are also included.

The example used to test the Power flow equations (PFE) solver is composed of central inverters. According to [2] this configuration is the most cost-effective nowadays despite the string inverters are close and present a series of benefits related with the versatility and control.

Contents

List of Figures

List of Tables

Acronyms

DES Distributed energy sistems. 19, 36, 37

ENSTO-E European Network for Transmission System Operators for Electricity. 33

eSCR Equivalent short circuit ratio. 40

LS-PVPP Large Scale PV power plant. 1, 4, 34, 37–40, 42–45, 47

MPP maximum power point. 19

MPPT Maximum power point tracker. 30

NRA Newthon-Raphson algorithm. 14, 16, 17, 24, 26, 51

PF Power factor. 5, 35, 38, 40

PFC Power factor control. 39

PFE Power flow equations. 1, 23, 28, 34

PoC point of connection. 5, 38–41

RfG Network Code on Requirements for Grid Connection applicable to all Generators. 33

SCR Short circuit ratio. 39, 40

TSO Transmission system operator. 33, 36

Chapter 1

Prefase

1.1 Objective

This work focuses of understanding and studying the collection grid and the energy distribution of solar photovoltaic plants (PV) in MATLAB. The main idea is to add a module to calculate the phenomena happening from the inverter to the point of couple to the grid. The present work starts from the results obtained by the model developed by Gabriele Catalano [1] and evolved by Eduard Foved [2].

1.2 Motivation

The present project follows the work done by Gabriele Catalano [1] and Eduard Foved [2] during their Master Thesis. Both of the mentioned projects are centered in the module to inverter part leading to black box models in the definition of other components functions such as the transformer or the grid itself. This work is an effort to develop a model to set optimal values and configurations for a better performance when exchanging energy with the transmission system and consumption centers.

The present work is an effort to review the state of art of the PV technologies and its integration in the different energy systems and in particular, the Spanish situation. The scope of the projects aims to cover the energy management requirements and their tendencies to introduce PV energy as a reliable source in the market.

Nowadays in a world of fast changes and climatic issues the environmental impact of the society should be taken seriously, consequently a deep research on the known effects of using PV technologies in a utility-scale is included in the project.

Chapter 2

Power flow analysis

The tool used in this work to analyse the parameters of all the buses and define the current flow are the power flow equations. For a given power network where the net apparent power and some other limitations or restrictions on voltages and power generations, solve for unknown bus voltages and generation and for the complex power flow in all of the network components.

2.1 Procedure

In the next section the steps followed to develop a power flow study for a generic network set by the user are discussed:

1. Obtain or determine the values of the passive network elements such as cable impedance parameters.

2. Set the location, measure the distances between members and find out the values of the complex power loads using tools as wattmeters.

3. Study every operator in order to set the generation specifications and constraints.

4. Design a mathematical model to model the power flow in the network.

5. Solve for the voltage of the network.

6. Solve for power flows as well as losses in the network.

7. Make sure the constraints set on the third step are not violated.

The fourth step is where the importance of power flow equations gains importance, they define the power flows of the systems and the resulting bus voltages, those are discussed in the following sections. As long as the system resulting from applying the equations is a nonlinear system with complex coefficients with as many unknowns as buses, the use of iterative methods or closed form techniques is mandatory.

2.2 Power flow equation basis

In this section the development of the power flow equations are briefly described to introduce the formulation that is explained in next section. The example where a number n of buses separated a distance by cables that introduce an impedance between them is used as a context to the development and is illustrated in figure (2.1).
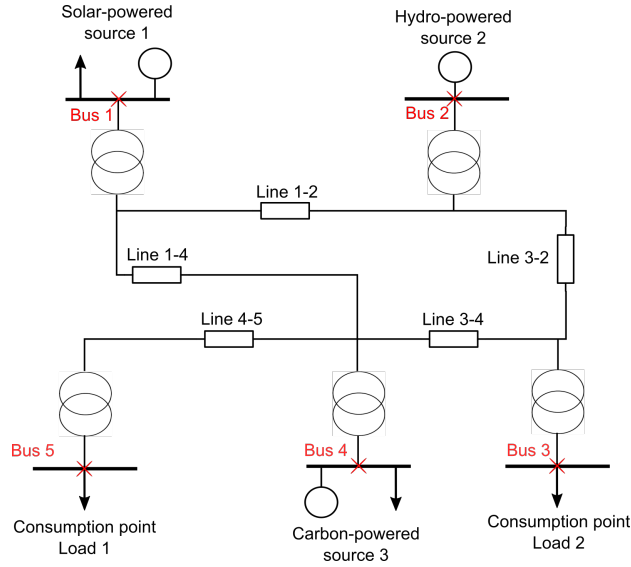
Figure 2.1: Example of a 5 bus system with the impedance of the lines.

The lines and the impedance of the buses are known and taking into account that the admittance is defined as:

$$Y = Z^{-1} \tag{2.1}$$

the bus admittance matrix is conformed. The detailed description is commented in section 2.3.

The Kirchhoff law is applied in every node yield resulting in expressions that describe the correlation between currents, obtaining equation (2.2) that can be applied in each node:

$$I_i = V_i Y_{i0} + \sum_{\substack{i=1, \\ i \neq j}}^{n} (V_i - V_j) Y_{ij} \tag{2.2}$$

Therefore expressed in a matrix environment the following relation results in:

$$[I_{node}] = [Y_{node}][V_{node}] \tag{2.3}$$

Where $[Y]$ is the admittance matrix, $[I]$ and $[V]$ are vector expressing current and voltage respectively for each node.

$$[I] = \begin{bmatrix} I_1 \\ I_2 \\ \vdots \\ I_n \end{bmatrix} \qquad (2.4)$$

$$[V] = \begin{bmatrix} V_1 \\ V_2 \\ \vdots \\ V_n \end{bmatrix} \qquad (2.5)$$

Introducing the relation expressed in (2.2) in the Gauss Power flow [I] that describes the apparent power as the voltage multiplied by the conjugate of the current and lastly regrouping terms the voltage can be described as

$$V_i = \frac{1}{Y_{ii}} \left(\frac{S_i^*}{V_i^*} - \sum_{\substack{j=1 \\ j \neq i}}^{n} Y_{ij} V_j \right) \qquad (2.6)$$

Finally considering that the apparent net power is defined by result of the power generated inside the bus and the power consumed by the load and the respective losses.

$$S_i^* = S_{gen-i}^* - S_{load-i}^* \qquad (2.7)$$

And if it is equaled to the Gauss Power Flow:

$$S_{gen-i}^* - S_{load-i}^* = V_i^* \sum_{k=1}^{n} Y_{ik} V_k \qquad (2.8)$$

The combination gives us a nonlinear equation system with implied difficulties, limitations and considerations that will be discussed later in this document.

2.3   Formulation

2.3.1   Bus admittance matrix

The Y matrix is defined by the admittance of the buses in the next configuration:

- The (k,k) elements are the result of the sum of the admittance of the elements present in the connection between node k and reference (Ground admittance $B/2$ and the admittance of the elements connected between nodes, the line admittance.

[I] $S_i = V_i I_i^*$ where i is the current node

- The (j, k) and (k, j) terms are defined by the negative of the admittance between respective j and k nodes.

A generic bus admittance matrix of a 3 bus network is shown in the next example:

$$[Y] = \begin{bmatrix} Y_{11} & Y_{12} & Y_{13} \\ Y_{21} & Y_{22} & Y_{23} \\ Y_{31} & Y_{32} & Y_{33} \end{bmatrix} \tag{2.9}$$

Examples of a (k ,k) and (j, k) components are shown next:

$$Y_{ii} = Y_{i0}{}^{\text{II}} + \sum_{\substack{j=1 \\ i \neq j}}^{n} Y_{ij} \tag{2.10}$$

$$Y_{ij} = -Y_{ij} \tag{2.11}$$

2.4   Limitations and considerations

This context introduce a number of difficulties in the calculations which are discussed next. The complex power outputs can be modified as long as the generation equals to the load in every bus. In fact the last generator calculated must be calculated last because it has to compensate all the uncalculated network losses, this is named the *Slack* bus. At the same time the losses are unknown until the voltages are calculated. In addition the flow is only valid for an arbitrary phase angle reference and it is not possible to solve the system for absolute values of angle or voltage.

For a example; for a four bus systems, in which one of the buses is the *slack* bus, the unknowns are voltages of all the buses plus the apparent net power of the *slack* generator. Therefore including the equation 2.8 evaluated for each bus it results in a system composed of four nonlinear equations with complex coefficients and five unknowns.

In order to solve the system using the mentioned iterative methods the *slack* bus voltage is specified. This way the number of unknown is reduced by one and the complex power generation is able to to fit the changes in both real and reactive power losses. The *slack* bus is also used as a phase reference with a limited magnitude. The next section will introduce the solution methods available as well as the procedure it follows.

2.5   Solution methods.

This section introduces the development of a correct solution as well as the different solutions proposed by the literature. In the present context there are four parameters of interest to know for each bus.

- Real power, associated from now with P.

$^{\text{II}}Y_{i0}$ is the admittance of the elements between node and reference or the i node.

- Reactive power; Q.

- Voltage module; V.

- Voltage phase; δ.

As it has been commented in every bus tools such as wattmeters are used to measure the values of the apparent net power S, therefore the P and Q values. The buses are classified in terms of the two known parameters, introducing the PV and PQ buses. Those are discussed in the definitions section.

The result of the application of the power flow equations in a real environment is a non-linear systems where the bus voltages and apparent power of the *slack* bus are unknowns. Different methods to solve nonlinear equations can be found in specialized literature, these are some:

- Gauss Seidel.

- Newton Raphson

- Fast Decoupled

There are some considerations to take into account; firstly these methods need guesses to start iterating and it is important to have good approximations. In order to evaluate the behaviour of the approximations a process is set and it is implemented in two stages; the first one calculates the approximate angles and the second the approximated voltage modules.

However the Gauss-Seidel is commonly used because the simplicity of the implementation and a better performance in front of the Gauss method, in this work the Newton-Raphson solution is chosen. The reasons are a fast convergence with a good initial guesses and a large range of convergence. Some disadvantages are the difficulties that the implementation brings implicit and the computing requirements resulting in an increment of the iteration step time. Newton-Raphson is a widely used method in the power flow analysis.

2.6   Definitions

In this section the items and concepts commented before are discussed in detail.

2.6.1   *Slack* bus.

A single bus for which the voltage and phase are specified designated to supply the unknown real and reactive losses, in consequence these values are unknowns. The selection of the *slack* bus depends manly on experience with the system under study because this bus must change to follow the variation in the losses to take up the slack. These decision has a significant influence in the results obtained.

ETSEIB

2.6.2   Load bus; PQ type.

This classification refers to the buses where the real and reactive power are specified. It is recommended to designate any bus with injected complex power as a load bus. The voltage magnitude and angle adapt to the situations created by the power injections. It has to be mentioned that the voltages have limitations to ensure smooth and secure voltage ranges for the devices connected to the grid. Usually these ranges go from 90 to 110% of the nominal voltage.

2.6.3   Voltage controlled bus; PV type.

As its name describes the voltage is controlled adding a voltage controller module that sets the voltage in a narrow range that can be understood as constant. In addition the real power is also specified. Consequently the reactive power is a variable with a limitations with upper and lower bounds. In a real situation a *PV* bus always have a generator that meets the requirements to be a variable source of reactive power.

2.7   The Newton-Raphson power flow solution.

2.7.1   Problem general form

In this section the Newton-Raphson algorithm is described; in the first part the presentation and general form of the problem are introduced. In the second part the matricidal power flow solution is discussed.

In practice, the bus apparent net power S_i is a parameter more accessible than the bus currents I_i therefore NRA reorganizes the equations following the next procedure. Regrouping terms the generic admittance expression is obtained:

$$Y_{ij} = |Y_{ij}|\angle\theta_{ij} = |Y_{ij}|\cos\theta_{ij} + j|Y_{ij}|\sin\theta_{ij} = G_{ij} + jB_{ij} \tag{2.12}$$

Using the Gauss power flow (2.8) S_i^* can be expressed as:

$$S_i^* = V_i^* I_i = V_i^* \sum_{j=1}^{n} (Y_{ij}V_j) \tag{2.13}$$

Now reorganizing equation (2.8) in correlation with the generic admittance reorganization (2.12) and the apparent power conjugate S_i^* equation (2.13) results the next expression:

$$S_i^* = P_i - jQ_i = \sum_{j=1}^{n} |Y_{ij}V_iV_j|\angle(\theta_{ij} + \delta_j - \delta_i) \tag{2.14}$$

Finally $2n$ equations are obtained following the generic form of:

$$P_i = |V_i|^2 G_{ii} + \sum_{\substack{j=1, \\ j\neq i}}^{n} |Y_{ij}V_iV_j|\cos(\theta_{ij} + \delta_j - \delta_i) \tag{2.15}$$

ETSEIB

$$Q_i = |V_i|^2 B_{ii} + \sum_{\substack{j=1, \\ j \neq i}}^{n} |Y_{ij} V_i V_j| \sin(\theta_{ij} + \delta_j - \delta_i) \tag{2.16}$$

The key idea behind the Newton-Raphson algorithm is to use a sequential linearization where function depending on x is equaled to zero. Starting from the initial guess every step an increment of Δx is defined:

$$f(\hat{x}) = 0 \tag{2.17}$$

$$\Delta x^{(v)\text{III}} = x - x^{(v)} \tag{2.18}$$

Representing $f(x)$ by a Taylor series where the components or 2nd order or higher are neglected. This can be done and performs well because the equation equals to zero. The expressions remains now as:

$$f(\hat{x}) = f(x^{(v)}) + \frac{df(x^{(v)})}{dx} \Delta x^{(v)} \tag{2.19}$$

Finally it can be solved for $\Delta x^{(v)}$ and start a new iteration setting the value of $x^{(v+1)}$ as the new one.

$$\Delta x^{(v)} = - \left[\frac{df(x^{(v)})}{dx} \right]^{-1} f(x^{(v)}) \tag{2.20}$$

This algorithm has a quadratic convergence meaning the error decreases quickly when approaching the solution and the result depends on the initial guesses that can be set for the voltages. Two are considered; $x^{(0)} = 0$ or $x^{(0)} = -1$. The iteration stop when the absolute value of the function with the current $x^{(n)}$ is lower than a tolerance, ϵ set by the user.

2.7.2 Multi-Variable NRA

The first change to notice is that in the multi-variable case the variables and functions $\hat{x}$, $f(\hat{x})$ and therefore the increment Δx become vectors containing the parameters for each bus. In addition the derivative component is now a matrix known as the Jacobian. This matrix contains the partial derivative of each function $f(\hat{x})$ for every variable x_n.

$$J(x) = \begin{bmatrix} \frac{\partial f_1(x)}{\partial x_1} & \frac{\partial f_1(x)}{\partial x_2} & \cdots & \frac{\partial f_1(x)}{\partial x_n} \\ \frac{\partial f_2(x)}{\partial x_1} & \frac{\partial f_2(x)}{\partial x_2} & \cdots & \frac{\partial f_2(x)}{\partial x_n} \\ \vdots & \vdots & \ddots & \vdots \\ \frac{\partial f_n(x)}{\partial x_1} & \frac{\partial f_n(x)}{\partial x_2} & \cdots & \frac{\partial f_n(x)}{\partial x_n} \end{bmatrix} \tag{2.21}$$

The system has a matrix structure therefore the operations must be performed in accordance. Following the solution scheme of previous sections the jacobian is inverted to solve for the increment Δx.

[III]v: represents the current step

The NRA application to power flow need a reformulation for the power equations associated to each bus. Taking in to account the equations (2.12) and the conjugate of (2.14) and defining the next expressions:

$$V_i = |V_i|e^{j\theta_i} = |V_i|\angle\theta_i$$

$$e^{j\theta} = \cos\theta + j\sin\theta$$

$$\theta_{ij} = \theta_i - \theta_j$$

The following equation can be obtained:

$$S_i = \sum_{j=1}^{n} |V_i||V_j|e^{j\theta_{ij}}\left(G_{ij} - jB_{ij}\right) \tag{2.22}$$

And resolving into the real and imaginary parts the equations used in the algorithm can be found.

$$P_i = \sum_{j=1}^{n} |V_i||V_j|\left(G_{ij}\cos\theta_{ij} + B_{ij}\sin\theta_{ij}\right) = P_{Gi} - P_{Di} \tag{2.23}$$

$$Q_i = \sum_{j=1}^{n} |V_i||V_j|\left(G_{ij}\sin\theta_{ij} - B_{ij}\cos\theta_{ij}\right) = Q_{Gi} - Q_{Di} \tag{2.24}$$

With the first bus designated as the *slack* bus and setting its voltage magnitude and angle the rest of the voltages and phases are found following the next scheme:

$$x = \begin{bmatrix} \theta_2 \\ \vdots \\ \theta_n \\ |V_2| \\ \vdots \\ |V_n| \end{bmatrix}$$

$$f(x) = \begin{bmatrix} P_2(x) - P_{G2} + P_{D2} \\ \vdots \\ P_n(x) - P_{Gn} + P_{Dn} \\ Q_2(x) - Q_{G2} + Q_{D2} \\ \vdots \\ Q_n(x) - Q_{Gn} + Q_{Dn} \end{bmatrix}$$

At the beginning of the iteration the number of steps is set to 0, $v = 0$ and the initial guesses are introduced. Each step the number is increasing in one, $v = v+1$ The stopping criteria is the same as seen before for a given tolerance, ϵ.

ETSEIB

PV cases

As long as the *PV* buses are fixed in voltage magnitude there's no need to include the unknown in the system or write the reactive power balance equations; it varies to maintain the fixed voltage within a reasonable limits. However those can be included writing the voltage constraint as $|V_i| - V_{isetpoint} = 0$. If they are not included in the system the script used in this work contains a simple limit violation test. It checks if the limits introduced in the bus data are violated. If the bounds are overpassed the program displays a message indicating which bus is having issues and the magnitude of these.

2.8   Load flows of the system

Once the NRA converged the Voltage magnitudes and angles are known and the line flows and losses are obtained.

First of all the Line Current Flows are calculated in each branch using Ohm's law in both directions of the branch. The resulting expressions are shown next: The *from bus-to bus* current expression is obtained:

$$I_{ij} = -(V_i - V_j a_{branch})Y_{ij}/a_{branch}^2 + b_{branch}/a_{branch}^2 V_i \qquad (2.25)$$

and the reverse direction expression results in:

$$I_{ji} = -(V_j - V_i a_{branch})Y_{ji}/a_{branch}^2 + b_{branch}V_j \qquad (2.26)$$

Where a is the tap setting and is set to 1 for all simulations. This tap setting is a functionality found in some transformers. It allows the transformer to have variable turn ratios to keep the changes of the primary side. The ground admittance is represented by b. In this work the ground admittance is the half of the susceptance present in any of the two buses conforming the line. Secondly, the Line Power Flows in MVA and the line losses are obtained using the apparent power equations:

$$S_{ij} = V_i I_{ij}^* * S_{base} \qquad (2.27)$$

$$L_{ij} = S_{ij} + S_{ji} \qquad (2.28)$$

Finally, the Bus Power Injections result from applying the equation (2.27) in addition to the initial bus current apparent power.

$$S_i^* = \sum_{j=1}^{Busn} V_i^* V_j Y_{ij} \qquad (2.29)$$

Where the real part is the active power $P_i = real(S_i)$ and the imaginary is the reactive power $Q_i = -imag(S_i)$.

ETSEIB

Chapter 3

Validating the results

3.1 Considerations.

In this chapter the process to validate the results is described and results of different cases are discussed.

The process of validating consist in considering different cases and running them in a consolidated power flow algorithm. In this work MATPOWER is set as the reference. The differences between the final results in both programs are discussed with the purpose of explaining them.

Once the reliability of the present work's program is set different scenarios are tested focusing on describing the behaviour of the system. The methodology for the analysis is based on varying the value of significant parameters of the system in a range that include realistic and common situations and observe the reaction of the power flows of the system.

The script contains different limitations that are commented in the next sections. Some of them are the reactive power limitation (Q_{max}, Q_{min}) when working with PV buses or the capability curve of the converters.

3.1.1 Limitations

In real situations there are a lot of physical limitations that can be easily missconsidered. The aim of this section is to cite all the limitations that have been taken into account and if it is possible define a procedure to deal with each one.

Capability curve of the converter

In the paper [2] the dependency of the inverter's capability curve on ambient temperature, solar irradiance, the dc voltage variation and the inverter operation. The converter used to perform the analysis found in [2] is an inverter formed by two stages; the first one is

a dc-dc stage used to step up the voltage to keep working on the maximum power point (MPP). The second one make the proper conversion to an ac signal.

The first two parameters, ambient temperature and solar irradiance, are environmental due to it the values can not be chosen. The rest of the parameters are electrical and can be modified with robust procedures. The dc voltage variation is limited in the lower limitation (V_{min}) by the minimum voltage to keep the ac side under the nominal values. These nominal values are dictated by the grid code applied. The upper limitation (V_{max}) in set by the open circuit voltage of each panel times the number of panels connected in series. In the figure (3.1) the relation between the V_{dc} and P_{dc} and the main points under study are represented.
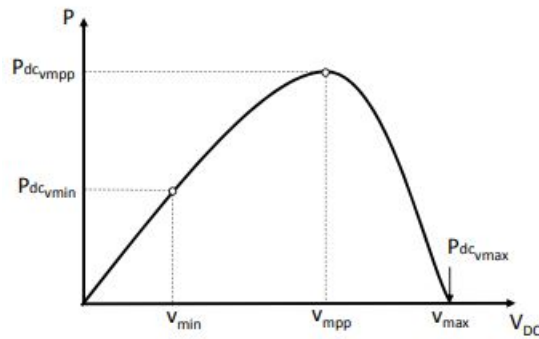
Figure 3.1: Relation between the P_{dc} and V_{dc} and main points to analyze.

3.1.2 Distribution system limitations

To ensure a correct and smooth penetration of the DES, especially solar energy based generation systems, many limitations are imposed. Depending on the definition of the buses, PQ or PV the remaining parameters have limitations. In first case the PQ achieve the given power values by regulating the voltage angle and magnitude. The boundaries and their strictness are set depending on the local point of the system and its possible implications on the devices connected to it. In section 4 the regulation and the examples of some grid codes can be found. In second case and analogously the PV buses maintain the voltage constant by regulating the reactive power. Thus, those are attached to the reactive power limitations that are explained in section 4

3.1.3 Parameters under study.

The indicators chosen to study and validate this work's results are listed next.

- Seventh bus angle and magnitude (V_{7thbus}): the capacitor is connected between the ground and the seventh bus therefore it is included is the analysis.

- Eleventh bus angle and magnitude ($V_{11thbus}$): both of the *surface script* and *linear script* impose the same changes in each of the four pv arrays (buses 11,12,13,14). Thus, the last bus included is the eleventh bus due to the balanced and symmetric grid in the present example.

- Second bus angle and magnitude (V_{2ndbus}): the second bus voltage is chosen due to the proximity to the connection point.

- Total active and reactive power demand.

- Total active and reactive power generation.

- Real and imaginary losses.

3.2 Example case.
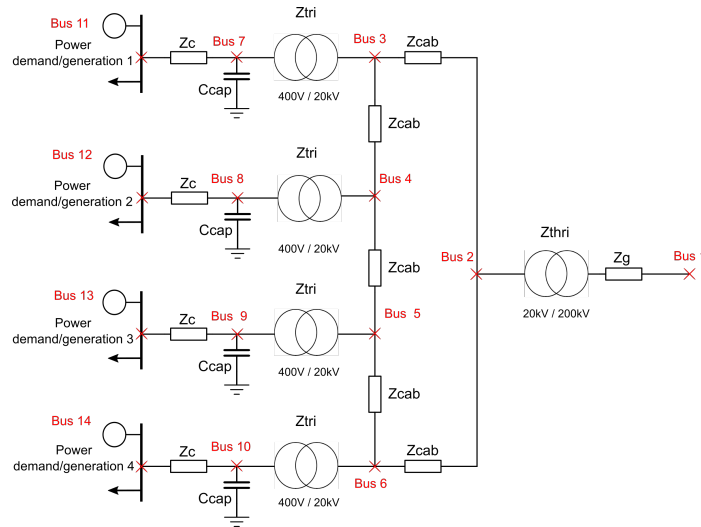
Figure 3.2: Example case with designated buses.

The figure 3.2 illustrates the system under study and the position of the buses. It remains the same for all the buses during all the scenarios.

The next table 3.1 contains the value of the different elements from the system

Table 3.1: Present work system parameters.

Element	Value
Rc	8E-03 ohms
Xc (4,28E-05 H)	1,345E-2 ohms
Xcap1 (4,20E-04 F)	7,5788 ohms
Rcab	1,475E-02 ohms
Xcab (1,42E-04 H)	4,446E-2 ohms
Rtr	1,60E-05 ohms
Ltr (1,45E-04 H)	4,5553E-02 ohms
Rtrhi	0,01 ohms
Ltrhi (9,55E-05 H)	3E-2 ohms
Rg	5,33E-02 ohms
Lg (1,697653E-03 H)	5,33E-1 ohms

3.2.1 Per unit values

The existence of transformers which have different ratio in the system make per unit values a great tool to work with. In order to change the values to per unit the base values shall be defined. The base apparent power remains the same in all the transformer sides. The base voltage is the one set by the transformer side where the impedance is located. Finally the relation between this base parameters and the current and impedance bases is set by the Ohm's law which is represented next:

$$S_{base} = V_{base}I_{base} = \frac{V_{base}^2}{Z_{base}} \tag{3.1}$$

With the *base values the conversion*[I] of all the values is performed resulting in the next table:

Table 3.2: Example's parameters in pu.

Z_{base1}	Z_c	(0,2 + 0,33615j) pu
	Z_{cap}	(-5,2778E-03j) pu
	Z_{tri}	(1,6E-07 + j4,5553E-04) pu
Z_{base2}	Z_{cab}	(1,475E-04 + j4,461E-04) pu
	Z_{thri}	(1E-04 + j1,152E-04) pu
Z_{base3}	Z_g	(5,333E-06 + j5,3333E-04) pu

3.2.2 Initial values and suppositions

As it is discussed in the Power Flow analysis section the script need some of the parameters to start a new case. In one hand in terms of the bus data the requirements are listed in

---

[I]$Z_{base1} = 0,04$ ohms, $Z_{base2} = 100$ ohms and $Z_{base3} = 10$ kohms.

ETSEIB

table (3.3).

Table 3.3: Required parameters for each bus.

Bus	Bus id
Type	1- Slack bus, 2- PV bus and 3- PQ bus.
V_{sp}	Voltage specified at the beginning for bus i.
theta	The V phase of bus i.
PG_i	Real power generated at each bus.
QG_i	Reactive power generated at bus i.
PL_i	Active power as load in bus i.
QL_i	Reactive power as load in bus i.
Q_{min}	Inferior limits for reactive power.
Q_{max}	Superior limit for reactive power.

In the first cases the following suppositions are assumed:

- The surface script is a method for validating the results against MATPOWER and there are no final conclusions extracted.

- The first bus is always the *slack bus*. In the current situation the grid bus is set as bus 1 and set as angle reference.

In the other hand the value of the lines is required. The parameters included are shown in table 3.4.

Table 3.4: Required parameters for each bus.

From bus	Bus id of the beginning of the line
To bus	Bus id of the end of the line
R [pu]	Resistance of the line.
X [pu]	Reluctance of the line.
B/2	Ground admittance
X'mer TAP	tap value.

The suppositions for the line parameters are:

- The Q_{max} and Q_{min}, in case of choosing *PV* buses, are set to -99 MVAr and 99 MVAr respectively that mean there are no limitations or those are considered wide enough for the systems power magnitude.

- The tap value[II] used to adjust the reactive power in the bus terminals is always equal to 1 in order to simplify the initial verifying operations and the existence of power electronics.

[II]the tap value is a capability some transformers have to change the turns ratio. It is used to manage the reactive power. Nowadays the power electronics are more efficient and much less cost-effective.

ETSEIB

- The ground admittance referred to the admittance of the shunt elements connected to the bus. The value refers to the half of the total susceptance (B) of the node due to the value is repeated in the two branches that include the particular bus.

3.3   Result comparison versus MATPOWER

With the aim of validating that the present work's PFE script is robust enough to extract conclusions of it, different cases are tested. Two MATLAB based programs are included in this work: the *surface script* and the *linear script*.

The *linear script* performs multiple simulations in both programs; PFE and MATPOWER changing one of the initial parameters and plots the results of the variables of interest discussed in section 3.1.3 in a 2D graphic. It is used to evaluate the effects of changing one of the inputs of the system with the aim of finding out its behaviour.

The *surface script* performs multiple simulations changing two of the initial values and plots surfaces representing all the combinations for a particular range of the two variables. It is used to validate the results versus MATPOWER. Both of them are limited due to the impossibility of applying different conditions on each PV array. However some cases will be performed manually, applying different conditions in some of the PV arrays (buses 11, 12, 13, 14). The *surface script* is useful to identify interest points such as minimum or maximum values depending on the two variables changing.

In the next sections a summary of the cases and the results for each program are discussed following the same structure:

1. Particular case initial values and considerations.

2. Result comparison.

3.3.1   First comparison: Active and reactive power demand variation with PQ buses.

Initial values and considerations

The reason for choosing the following parameters is discussed in the section 3.1.3. This case is conformed to test the capability of the PFE solver to work with PQ buses.

The values used for the simulation are shown in the next table and are referenced to the buses 11, 12, 13 and 14. In the real system these buses represent the PV arrays into the collection grid:

Results

Firstly the results for the voltage and angle of the buses of interest are displayed in figures 3.3, 3.4, 3.5. The original colors are black with 60% of opacity and green. As the results

ETSEIB

Table 3.5: Selected variables and ranges

Variable	Range
Active power demand [MW] (P_l)	[0.2, 0.6]
Reactive power demand [MVAr] (Q_l)	[0.1, 0.3]

are exactly the same the surfaces are overlapped and the resulting color is a mixture between them.

Once the values for voltage from the NRA are validated the load-flow solution is performed in both programs. The result comparison can be found in section 6.5.

ETSEIB

(a) 11th Bus magnitude

(b) 11th Bus angle

Figure 3.3: Eleventh bus values (1st case)

(a) 2nd Bus magnitude [p.u.]

(b) 2nd Bus angle [°]

Figure 3.4: Second bus values (1st case)

(a) 7th Bus magnitude

(b) 7th Bus angle
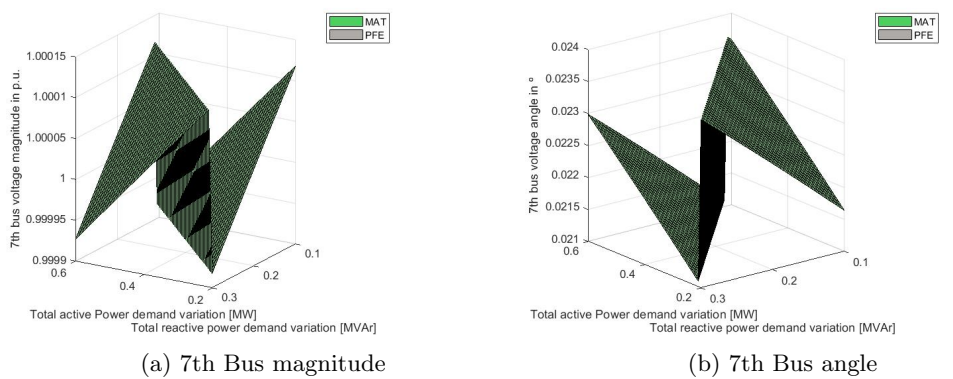
Figure 3.5: Seventh bus values (1st case)

3.3.2 Second comparison: Active and reactive power generation variation with PQ buses.

Initial values and considerations

The values used for the simulation are shown in the next table and are referenced to the buses 11, 12, 13 and 14. In the real system these buses represent the PV arrays into the collection grid:

Table 3.6: Selected variables and ranges

Variable	Range
Active power generation [MW] (P_l)	[0.2, 0.6]
Reactive power generation [MVAr] (Q_l)	[0.1, 0.3]

Results

Firstly the results for the voltage and angle of the buses of interest are displayed in figures 3.6, 3.7, 3.8. The original colors are black with 60% of opacity and green. As the results are exactly the same the surfaces are overlapped and the resulting color is a mixture between them.

Once the values for voltage from the NRA are validated the load-flow solution is performed in both programs. The result comparison can be found in section 6.6.

ETSEIB

(a) 11th Bus magnitude
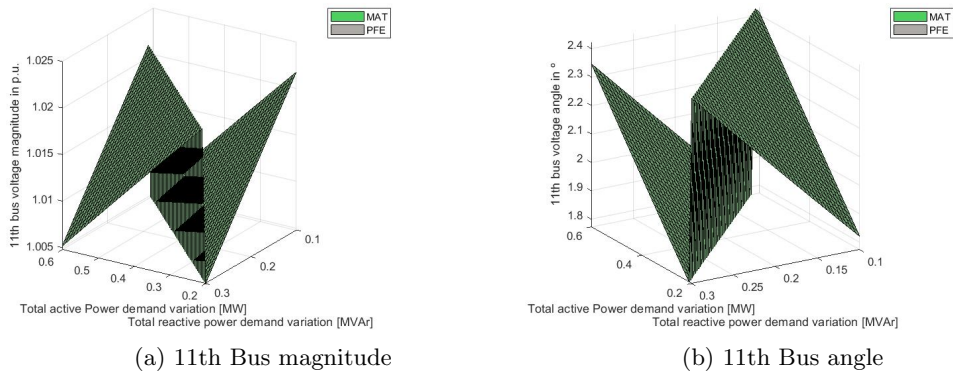
(b) 11th Bus angle
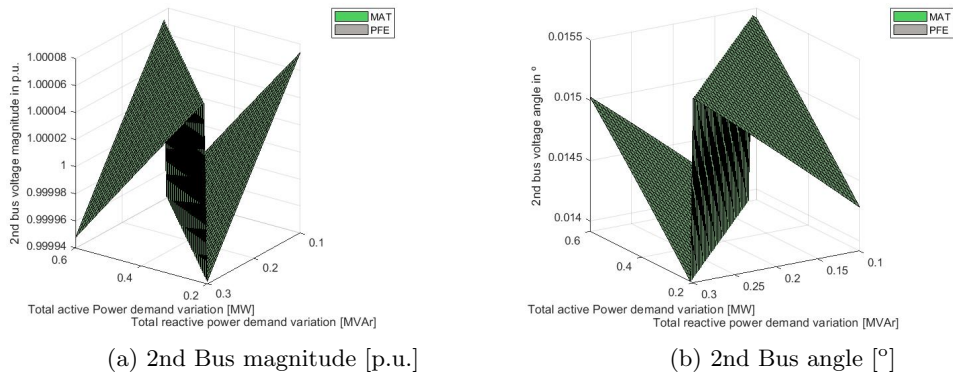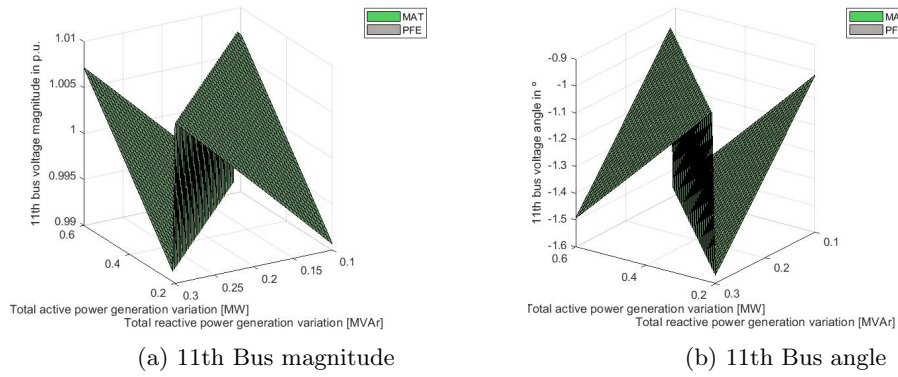
Figure 3.6: Eleventh bus values (2nd case)

(a) 2nd Bus magnitude [p.u.]

(b) 2nd Bus angle [º]
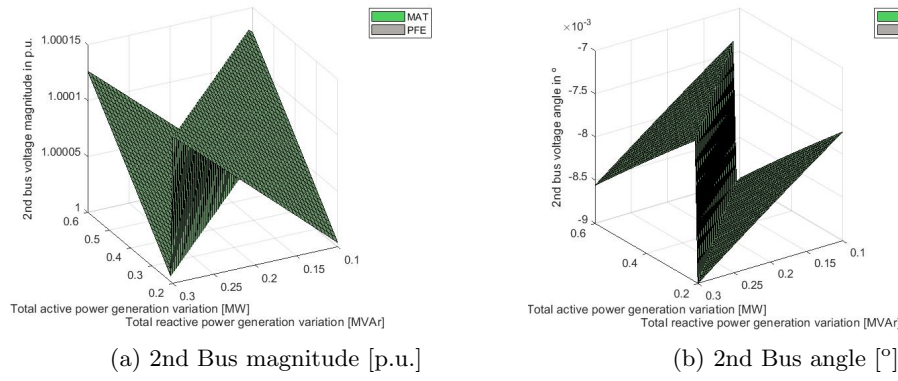
Figure 3.7: Second bus values (2nd case)

(a) 7th Bus magnitude

(b) 7th Bus angle
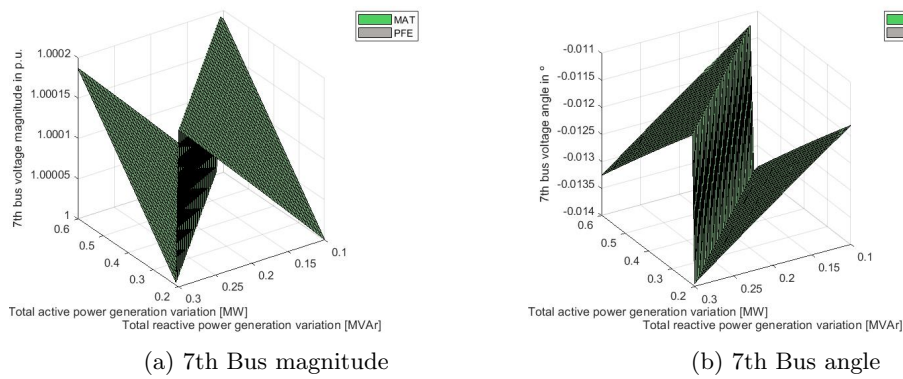
Figure 3.8: Seventh bus values (2nd case)

3.3.3 Third comparision: Active power generation and grid voltage variation with PV buses.

Initial values and considerations

This test is performed to test the capability of the PFE solver to work with PV buses.

The values used for the simulation are shown in the next table and are referenced to the buses 11, 12, 13 and 14. In the real system these buses represent the PV arrays into the collection grid:

Table 3.7: Selected variables and ranges

Variable	Range
Active power demand [MW] (P_l)	[0.2, 0.6]
Grid voltage [p.u.] (V_1)	[0.95, 1.15]

Results

Firstly the results for the voltage and angle of the buses of interest are displayed in figures 3.9, 3.10, 3.11. The original colors are black with 60% of opacity and green. As the results are exactly the same the surfaces are overlapped and the resulting color is a mixture between them.

The specified voltage for the PV buses (buses 11, 12, 13 and 14) is 1 as it can be confirmed in figure 3.9a.

Once the values of the iteration are confirmed the load-flow solution is performed in both programs. The results can be found in section 6.7.

ETSEIB

(a) 11th Bus magnitude

(b) 11th Bus angle
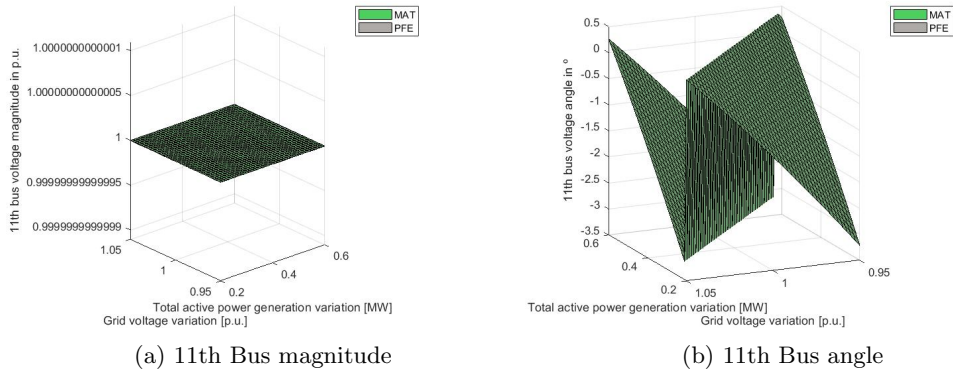
Figure 3.9: Eleventh bus values (3rd case)

(a) 2nd Bus magnitude [p.u.]

(b) 2nd Bus angle [°]

Figure 3.10: Second bus values (3rd case)

(a) 7th Bus magnitude

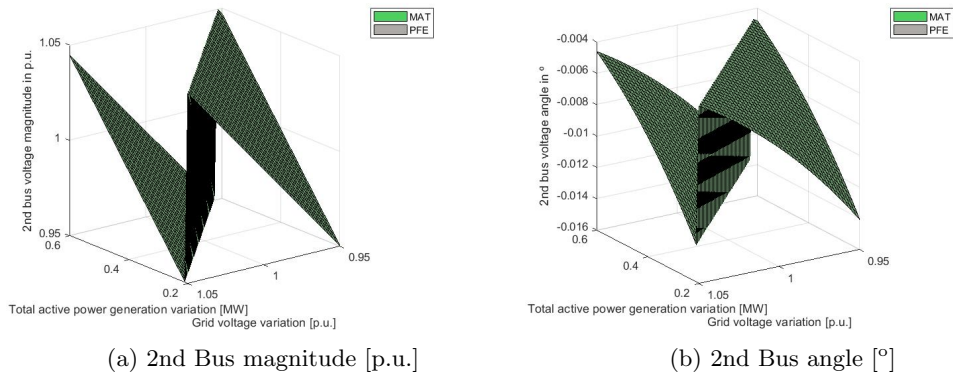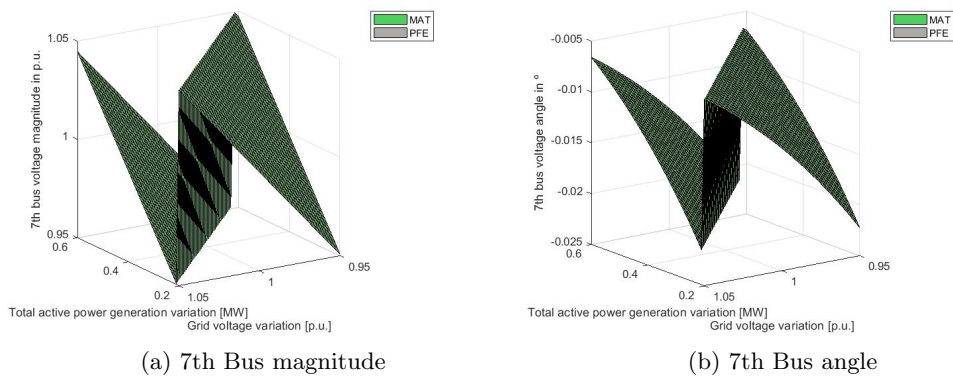(b) 7th Bus angle

Figure 3.11: Seventh bus values (3rd case)

3.4 Analysis of maximum and minimum voltage deviations and loses.

In this section individual simulations and are performed with the aim of defining the behaviour of the system. For the next simulations all the converter outputs are set as PV type buses as the majority of devices need a range of voltages to work correctly and the magnitude of the changes in the system's voltages are commonly wider than those ranges. In section 4.3 a new type of bus is defined where the reactive power is a function of the voltage with the aim of reducing the losses and therefore the stress of the system among other benefits.

3.4.1 Particular case: different values for each converter output

In this case the voltage of the converters (buses 11, 12, 13 ,14) are set to different values to simulate a real situation where the differences between components and conditions set different efficiencies in each PV array. For example; different dust densities in the panels or shades that reduce the efficiency of the Maximum power point tracker (MPPT)[III]. The initial data for the buses is summarized in the table 3.8 Using the script *Individual*

Table 3.8: Initial values for the converter output buses.

Bus id	Voltage [p.u.]	P demand [MW]	P generation [MW]
11	1.02	0.65	0.43
12	1.01	0.59	0.44
13	1.03	0.62	0.41
14	1.09	0.66	0.40

case the results are obtained and represented in figure 3.12. It can be observed that the maximum voltage deviation in per unit, excepting the voltage regulated buses, is found in bus 5 with an increment of 0,0161% which transformed to real values is an increment of 322 V. The minimum voltage deviation is found in bus 2 with a per unit increment of 0,0094% and real value of 188 V.

The losses and injected apparent powers in each bus are illustrated in figure 3.13. The real and imaginary losses are similar to the magnitudes of the*surface script* for the same grid voltage value and active power generation figure 6.10. In fact if the *linear script* is used to evaluate the relation between the grid voltage and both imaginary and real losses using the same initial data. The results from figure 3.14 correspond to a variation in grid voltage from 0.9 to 1.1 p.u. It can be concluded that both losses present a minimum when the grid voltage is 1.

[III]MPPT: is a device that set the voltage in the array to meet the maximum active power output. It has to work with the lower voltage on the array therefore if one panel is performing poorly the rest of the array is affected. It is considered as a type of loss.
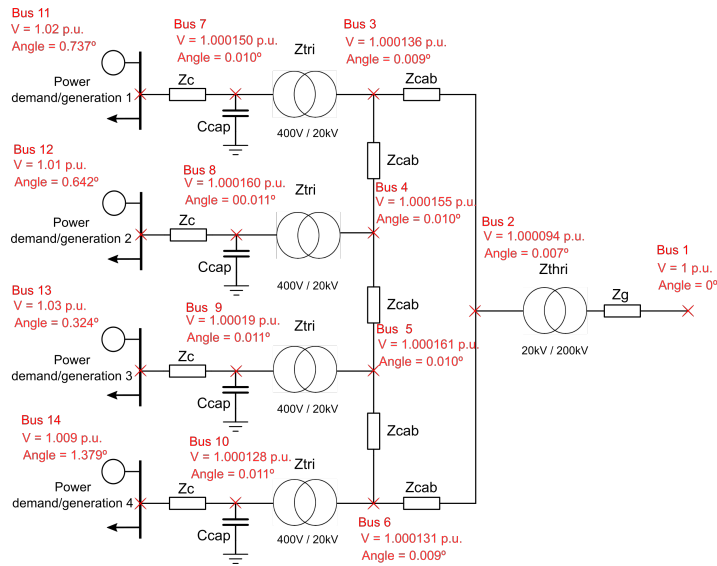
ETSEIB

Figure 3.12: Example scheme with voltage magnitude and phase values

Figure 3.13: Example scheme with voltage magnitude and phase values
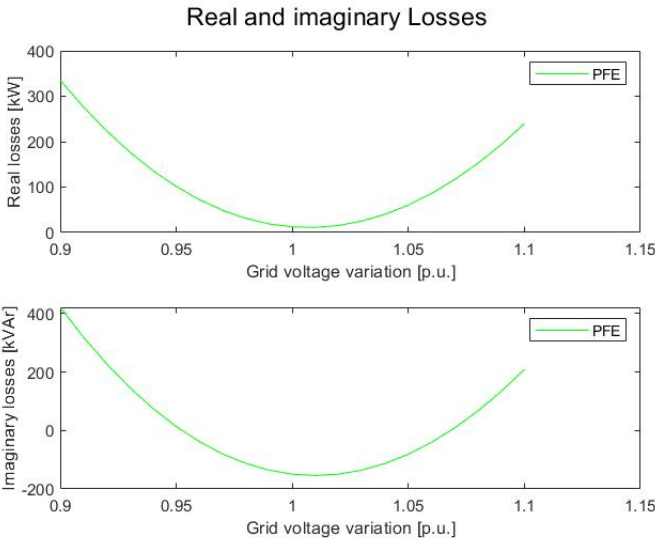
Figure 3.14: Real and Imaginary losses changing the grid voltage from 0.9 to 1.1

Chapter 4

Grid code requirements

4.1   Introduction

A Grid Code is a technical document containing the rules governing the operation, maintenance and development of the transmission system. It is necessary due to the existence of different energy suppliers that work with the same Transmission system operator (TSO). In the grid code all the requirements are specified and discussed to ensure stability and quality of electrical systems in continuous operation as well as during fault's or extraordinary events. Grid codes are different and depend on the country they are conformed. Each country elaborates one and the differences between them are motivated by the characteristics of the country and the particular needs created by the local electrical system. However according to [7] there is a tendency to harmonize grid codes in different EU countries with documents such as: Network Code on Requirements for Grid Connection applicable to all Generators (RfG) drafted by European Network for Transmission System Operators for Electricity (ENSTO-E). These documents are used as framework while developing grid codes.

The increasing penetration of renewable energies during the last decades have forced improvements in the technology and system's behaviour control. These changes are mainly motivated by the intrinsic characteristics of renewable energies, such as the dependency on the environment and the intermittent behaviour of the natural energy resources. These variations can conclude in undesired faults creating damages to the transmission system elements and all the equipment connected to the network. The grid codes are constantly updated to ensure smooth and correct functioning in all situations.

For example the grid code of a large country with a good number of sources and a low penetration of renewable energies must have less strict conditions for transmission system frequency than a little island which has an equal proportion of renewable and non-renewable energy sources.

There are two types of requirements: static and dynamic. Static requirements refer to the continuous operation state and the dynamic collect the procedures to follow during fault sequences and disturbances. The grid codes include *worst case scenarios* to cover

all the possible events that can take place including strict measures as the complete disconnection.

The renewable energies present a big flexibility to penetrate in the market as they can be introduced as wind farms, PV plants, Hydro-powered stations... The solar energy is one of the resources that are experiencing a fast growth during the last decades. In the paper [6] presented in MPDI journal it is exposed that the power installed capacity in Spain for solar energy increased over a 5 GW from 2007 to 2018 with a positive tendency. The evolution is represented in figure 4.1.
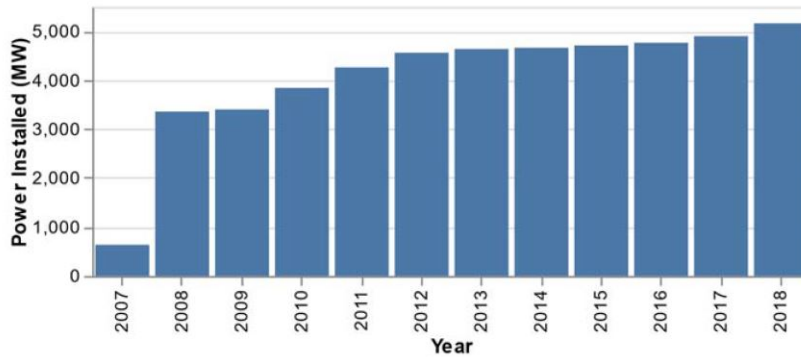
Figure 4.1: Power installed in Spain from 2007 to 2018.

In the present work the grid code requirements for a Large Scale PV power plant (LS-PVPP) are discussed and contextualized for different grid codes. The particular solution presented in [8] for compensating reactive power is introduced in the present work PFE solver.

According to [11] the amount of energy managed via the peninsular system's ancillary services in GWh is illustrated in figure 4.2.

	2017		2018	
	Upward	Downward	Upward	Downward
Technical constraints (PDBF)[1]	11,035	739	10,969	374
Secondary control	1,203	1,206	1,086	1,506
Tertiary control	2,348	1,806	1,913	1,118
Deviation management	1,006	760	1,883	475
Real-time technical constraints	207	434	172	290
Total energy managed	20,746		19,785	

Figure 4.2: Summary of the total energy managed by the ancillary services in the spanish peninsula.

ETSEIB

4.2   Static regulation

In general the static regulation for renewable energies depend on the resource used and its intrinsic characteristics. For example for solar and wind sources power curtailment is needed due to the unpredictable availability and the fast and wide variations they can suffer due to environmental conditions. Power curtailment limits the power extraction in two different situations: when the power extracted is greater than the nominal value of the plant in peak generation events or when the demand is lower than the production.

In [4] an analysis of the connection requirements of wind power generation units for six grid codes is carried out.

4.2.1   Power factor regulation

The power factor is the ratio of reactive to apparent power consumption, thus its requirements and the reactive power are similar in the different Grid Codes. Any inductance with no capacitors attached consumes reactive power. Consequently this reactive power consumption must be produced somewhere in the grid. One thing to consider is that the distribution of reactive power is cost intensive and the reactive power is not profitable although it is used in some cases to support the grid during particular events. In [5] an example of different Grid Codes power factor/reactive power requirements is presented:
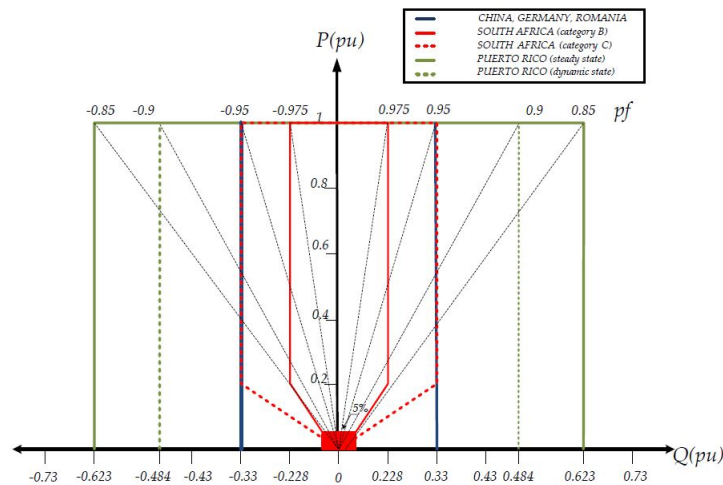
Figure 4.3: Reactive power requirements for Puerto Rico, South Africa and China, Germany and Romania.

The most restrictive PF requirement in figure (4.3) is the red line referring the Grid code from South Africa. From 100% to 20% of production the maximum PF are 0.975 leading and 0.975 lagging.

One of the limitations commented in section 3.1.1 are the reactive power bounds for PV buses. Those limitations should be established in order to meet the Grid Code guidelines

of reactive power consumption.

4.2.2   Power Curtailment

Power curtailment introduces the possible reduction of generated active power depending on grid requirements. Two common situations where power curtailment is effective are:

- The possible overloading at peak generation hours for natural resources as wind or solar energy. Due to the inherent characteristics of those.

- When the demand is lower than the generated active power without power curtailment.

The overloading is regulated by the TSO because it would cause an increment of the frequency, therefore an increment in the inertia of the transmission system.

The power curtailment is not outlined precisely in most of the Grid Codes and it depends on environmental conditions, installed capacity and economics. According to [4] an indicator to apply this requirement is the frequency surplus. In European countries, with a grid frequency of 50 Hz, the bound to start applying power curtailment was 50,5 Hz. When the frequency deviation decreases the reestablishment of the active power has its own limitations. It should be less than the 10% of the network capacity per minute. Figure 4.4 extracted from [4] illustrates the operation conditions when the network is overloading.
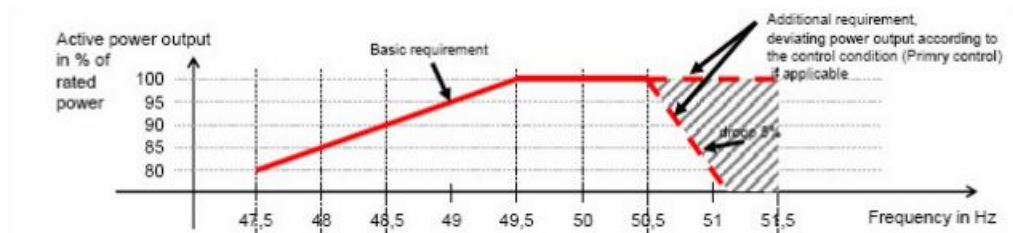
Figure 4.4: Power curtailment requirements

4.2.3   Active power reserves

The tendency of introducing more and more Distributed energy sistems (DES) based on renewable energies in existing distribution networks generates new problems. The difficulty of prediction and intermittency of renewable energy sources in addition to the high density of DES lead to voltage and frequency issues in the distribution network. For example the proximity of PV plants due to the land restrictions submit them all to the same environmental conditions. It has to be noticed that the most common peaks of solar production are found in the middle of the day where the demand is low. The energy surplus is redirected into the grid however in a distribution network with a high density

of DES it can conclude in bidirectional power flows, overloads or over voltages on some branches or transformers.

To fix this issues and ensure a smooth penetration of the DES in the distribution networks two solutions are found. The first one is the use of batteries as energy storage systems to supply the active power demand in compromised situations. Although it has been experimentally implemented presenting good results it is still cost-prohibitive and is not cost-competitive if compared with other sources. The main problem is the current energy storage technology that presents a low efficiency and a high maintenance and production costs at this power ratings. The alternative method is the active power regulation. It is based on the power curtailment. In a situation where the energy production can reach the nominal values the active power output is regulated to offer around an percentage of the maximum capacity. The remaining capacity is set as active power reserves. This approach is easier to implement but it causes a reduction in the efficiency of the plant.

4.2.4 Voltage range and Control

The PV plant must be able to run at rated voltage plus the specified voltage range. The rated voltage and the voltage range varies depending on the transmission system, which depends on the country. The voltage ranges at the different rated values, for limited periods of time during fault or particular events, are also specified. According to [4] the requirement for all nominal values in continuous operation varies around $\pm10\%$ of the nominal value.

4.2.5 Remote Voltage Control

Additionally in most of the grid codes it is required that the LS-PVPP or power station contains a closed loop voltage regulation system.

The voltage regulation follow the basis of the PV bus definition where a voltage set point is specified and regulated by continuously modulating the reactive power output in the acceptable ranges. In addition the voltage set point shall be within the limits.

The time response of the voltage regulation system is also specified in some of the grid codes analyzed in [4].

4.2.6 Frequency

The generator's plant must be capable of working in accordance with specified frequency ranges. The majority of the grid codes presented [4] must be able to run continuous operation in frequencies between 47,5 Hz and 52 Hz. Time delays might be necessary in some range of frequencies. The procedure in case of breaking the limits is to reduce the active power output and remain connected. Disconnection is only permitted at frequencies below 47 Hz and above 53 Hz and with no time delay.

ETSEIB

4.2.7 Flicker

A flicker is a single, rapid change of the root mean square voltage. The connection of different elements such as capacitors, lines, cables, transformers and other elements may cause transmission system step changes.

It must be mentioned that a lot of grid codes do not mention flicker's, according to [4] the Danish grid code specifies the next procedure.

Different thresholds are set depending on the time interval where the flicker magnitude is evaluated. The short term flicker is a weighted average of the flicker contribution over ten minutes. The long term flicker is defined over 2 hour.

Finally in figure 4.5, extracted from [5], a summary of the requirements for a LS-PVPP is illustrated for a better understanding.
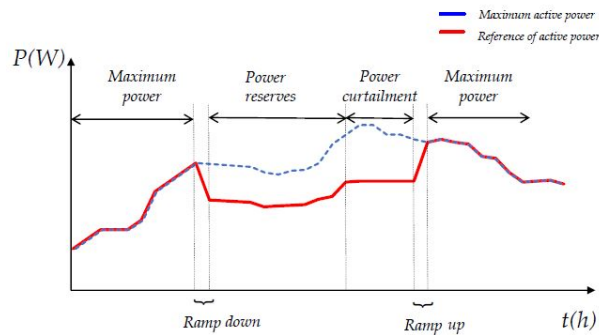
Figure 4.5: Summary of grid codes requirements for LS-PVPP

4.3 Grid support; reactive power compensation

As the present work is centered in renewable energies and they are based on natural resources usually the generation plants are located in remote areas. Consequently the transmission lengths are long enough to consider the transmission line impedance significant. As the transmission lines are mostly composed of inductance elements, which are part of the imaginary domain, and transformers.

The inverter is synchronized to a point of connection (PoC) and the feedback measurements are taken at this point. As the current fed to the PoC flows through the grid impedance a quantity of reactive power is created although the inverter is working at unity PF. Thus, the active power of the PV inverter becomes coupled with the reactive power seen by the grid. This undesired reactive power causes a bad behaviour that includes an increase in transmission losses and consequently reduces the maximum transmission capacity, compromises system stability and strains the grid.

The undesired reactive power depends on the grid current and grid impedance. If the impedance is high the PoC current has a significant impact on the local voltages. A grid

ETSEIB
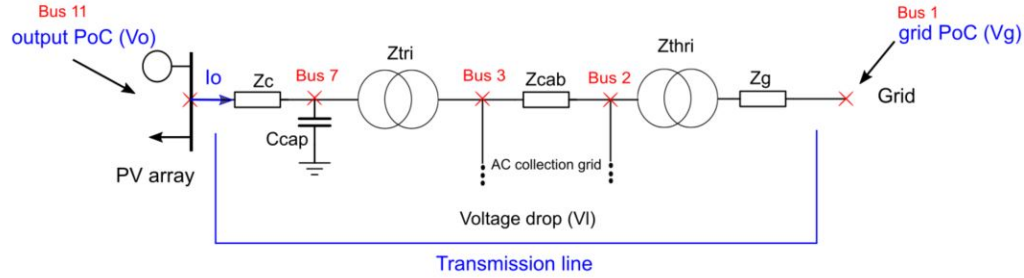
Figure 4.6: Scheme of the connection points contextualized in the current example

with a high impedance is defined as a *weak grid*. A parameter to measure the degree of weakness is the Short circuit ratio (SCR) which is defined by the next expression:

$$SCR = \frac{V_n^2}{S_n Z_g} \tag{4.1}$$

Where V_n is the nominal voltage, S_n is the nominal apparent power (usually in distribution generation systems is the value of the inverter due to the transformers have the same power ratio) and Z_g is the transmission system impedance. Once the value of the SCR is less than 5 it can be considered weak. As it is commented in previous sections the renewable energy generating plants are located at remote locations the impedance become significant, thus the grid is considered weak.

According to [8] the reactive power has been managed using synchronous generators, capacitor banks as the present work case examples or with FACTS[I] devices. The reactive power of an inverter is relatively easy to control without the need of additional investments.

The reactive power control has two goals: voltage regulation and reactive power optimization or a compromise between them. In fact they can not be optimized simultaneously as they are related. In [8] and in the present work the voltage regulation is not considered as the buses are set as PV buses and a notification pops up if the Q limits are violated with the current voltage setpoint.

According to the authors of [8] the most common approach to control reactive power in LS-PVPP is the Power factor control (PFC) where the reactive power is proportional to the active power feed. Conventional PFC assumes the active power-reactive power ratio (Q/P) constant although the reactive power injection from inverter affects the PoC voltage changing the commented Q/P ratio and therefore the PFC achieves optimal decoupling only when the inverter is operating at nominal values. In renewable generation systems the active power output changes drastically along with the environmental conditions therefore if traditional PFC is applied it leads to suboptimal reactive power compensation.

[I]FACTS: flexible alternating current transmission system: system of static components used for the AC transmission used to enhance control and increase power transfer capability for the network. It is usually based on power electronics.

In [8] a method for autonomous compensation of undesired reactive power flow from the transmission line reactance is presented. It includes a continuous-real time impedance measurement is used to estimate the transmission reactance. Based on the outputs and the commented estimation the undesired reactive power is compensated and consequently the active power from the PV inverter is decoupled from the reactive power seen by the grid. It allows the reactive power of the inverter to be controlled and still set the reactive power value to 0 in the grid side. In the present work the estimation of the impedance is not used as the grid parameters are known; for more information in [8] the estimation method is widely discussed. In conclusion the present work's goal for grid support is to decouple the reactive power drawn from the grid that decreases the PF.

An image extracted from [8] illustrates the differences between the phasor at the different points of connection:
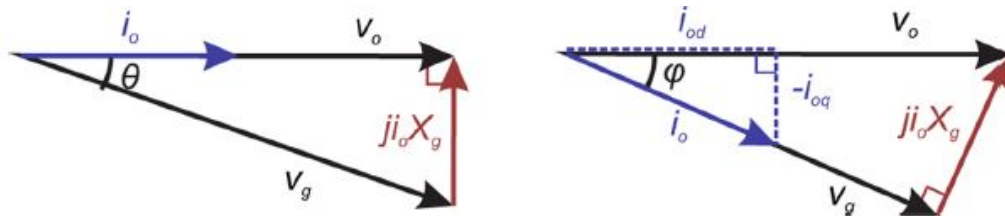
Figure 4.7: From left to right; output PoC and grid PoC phasor diagrams when PF is set to unity.

As it is noticed when connecting to the output PoC with the inverter working at unity PF the output current is in phase with the output voltage. On the grid side and after passing through the transmission impedance the current and output voltage are shifted, thus the grid side PF is reduced. The reactive power compensation can be performed directly by adjusting the output's voltage angle to match the grid voltage angle. In conclusion if the compensation is applied the grid's PF shall be equal to unity.

The wide and fast fluctuations of the renewable resources cause changes in the active power which result in a variance of the reactive power consumption related with the transmission system. In the present work the LS-PVPP are supposed to be weak grids, thus these active power variations can cause an undesired reactive power flow; increasing transmission losses and limiting the active power of the line. These events can conclude in compromising the system stability. If the reactive power changes the power angle beyond a limit the equilibrium point no longer exists and the system becomes unstable.

In the context of the renewable energies another indicator for evaluating the stiffness of the grid is set. The Equivalent short circuit ratio (eSCR) follows the same concept than the SCR but it takes the instantaneous power instead of the nominal. With this change being applied the fluctuating nature of the active power is covered.

Compensation of the unintended reactive power.

The unintended reactive power flow can be compensated by forcing the inverter's output current angle to match the grid PoC voltage angle. According to [8] the transmission line consumes a reactive power of Q_g with a total transmission reactance X_g while the capacitive filter used to compensate produces a reactive power of Q_c. Thus the total reactive power Q_{total} follows the next expression for one line:

$$Q_{total} = Q_g + Q_c = I_o^2 X_g - \frac{V_o^2}{X_c} \tag{4.2}$$

Where I_o and V_o are the current and voltage outputs of the converter.

Chapter 5

Environmental impact analysis

In this section the environmental effects of a LS-PVPP and its distribution system, its components and the control methodology are discussed. The object of the study tries to focus on renewable energies as generators due to the restrictions they are attached in terms of location and availability of the natural resource. In the scope of this project are included the impact on the landscape, the side-effects suffered by the wildlife and the possible impacts on the society.

The present project is centered in solar energy and the conclusions are particularized for this natural resource. However many of the conclusions can be extracted for other energy generation methods. The analysis is divided by areas. Each area is centered in a period of the lifetime of the PV plant. Usually a LS-PVPP has a functional period that varies between 25 and 40 years.

As it is discussed in [9] there are diverse benefits of solar energy implementation in a particular location. Those include the reduction of the greenhouse effect gases, the stabilization of the degraded land and the increase of energy independence among others. It is important to notice that the creation of a PV power plant introduces social benefits as well, the acceleration of rural electrification and the creation of job opportunities.

5.1 Large scale PV power plant

Solar energy is one of the best looking alternatives to fossil fuels in terms of fighting the climate change. The table 5.1 contains values extracted from [9] comparing solar energy technologies and conventional production systems. The *photovoltaic* systems present ten times less contribution to the climate change than a conventional carbon-intensive system. Indeed a breakdown of the generation structure of the peninsular system extracted from [12] shows the tendency to substitute dirty sources of energy. Between 2017 and 2018 the total generation percentage of the peninsular system went from 33.7% to 40% with a 3% of solar energy share.

Table 5.1: Comparison of life cycle emissions for solar technologies and conventional carbon-intensive systems

Conventional systems		Renewable systems	
Production system	g-CO_2/kWh	Production system	g-CO_2/kWh
Coal	975	Crystalline-silicon	45
Gas	608	Thin-film amorphous silicon	45
Oil	742	Thin-film cadmium telluride	14
Nuclear	42		

Solar energy land use is smaller than average land use presented by other energy systems including renewable sources as wind. Furthermore the changes introduced by solar energies are less intense. In fact solar energy brings with it co-benefit opportunities. Some of them are the utilization of degraded lands, the mixture between solar panels location and agriculture or hybrid power systems.

In the following sections some of the possible effects of the solar energy implementation are discussed. Firstly classified depending on the stages of the life cycle of a PV power plant and then depending on the affected medium.

5.1.1 Construction

The magnitude of the demand of a utility-scale PV plant is usually around megawatts, consequently a wide area is needed to achieve that power generation. At first sight it can seem a minor inconvenient but the land restrictions, applied in order to protect the natural environment and reduce the landscape impact, in addition to the inherent characteristics of solar energy such as the inttermitency and the local availability of the resource reduce drastically the available terrain.

The construction stage includes actions as vegetation removal and complementary operations such as the creation of new roads, corridors and the transmission lines. These operations can have negative effects in the environment due to the landscape impact and noise and light pollution that can affect to the biodiversity in a wide spectrum of ways.

5.1.2 Operation

In this stage different maintenance operations are performed. The dust affects directly in the efficiency of the PV panels therefore a cleaning routine needs to be done. The roads used to access the panels and perform the different operations are already built. It is important to notice that LS-PVPP needs energy to start generating and this energy can come from non renewable sources. Thus, this energy can be summarized in equivalent CO_2 emissions.

ETSEIB

5.1.3   Decommission

In the decommission stage the PV cells shall be recycled in order to avoid toxic substances including cadmium, arsenic, silica dust and chemical products such as dust suppressants, coolant liquids and herbicides among others. Those substances are very toxic and in case of inappropriate handling can pollute surface ground, superficial water accumulations and aquifers.

5.1.4   Potential environmental consequences

The use of environmental toxicants and flammable products is constant during all the stages. A procedure to neutralize those substances needs to be established if possible. The vehicular activity and soil disturbance are permanent effects during the lifespan of the PV plant.

Different environmental implications are related with the installation of PV power plants. Some of the more significant changes in the environment are commented next. The changes in albedo along the PV panels consumption lead to changes in the surface temperature and the precipitation regime which can be summarized in changes in the microclimate and local hydrology. More information can be found in [9].

5.1.5   Potential ecological consequences

Land level effects

All the changes commented before can lead to a ecological response that includes a wide impact on the biodiversity and soil nutrients dynamics. Usually LS-PVPP are located in remote areas where there is a wide biodiversity and the related footprint changes completely the environment during the lifetime of the plant. The removed vegetation serves as air filter in many scenarios especially in arid terrains; it retains dust and sediments traveling with the wind, from dispersing around. Those sediments directly affect the efficiency of the PV plants by simply accumulating in the PV panels or absorbing some of the irradiance coming from the Sun while suspended in the atmosphere.

The PV panels operational maintenance includes panel washing in order to maximize the efficiency. The process of cleaning the panels is manly based in water which can be an issue in some arid territories or places where water is an scarce resource.

The wide area occupied by the LS-PVPP create barriers to the genes spreading of certain species with little-range movement patterns that are not able to circumvent the installation. Repatriation and translocation programs consist in collect the affected species and release them in different areas. However, according to [9], those methodologies have a low success rate close to 20% due to the complications of some species to adapt and overcome in new environments with an existent ecosystem. Another mitigation methodologies have been tested but the cost and the individual requirements of each specie do not guarantee benefits. In addition some species as birds can not be controlled and they suffer accidents

related with the infrastructure. Changes in the land distribution, vegetation and biodiversity in addition with the creation of roads which increments accessibility allow invasor species to move in.

Land-atmosphere synergies

PV panels have an effective albedo between 0,18 and 0,23 that is above the average albedo for the rural areas where the LS-PVPP are located. It concludes in an increase of the soil surface temperature that can affect environmentally sensitive ecosystems. A high density of PV generation can cause a change in the radiative balance that can not be understated.

5.1.6 Transmission system impact

The need of long transmission lines to transport the energy generated at the power plants to the population centers where the consumption occurs as a big environmental impact. The major problem is centered in the land use; for example in [9] is said that only in 2007 more than 300 km of high-voltage transmission lines where constructed in the United States. Nowadays, in an energy market that is constantly growing and diversifying, new opportunities related with more efficient and robust renewable technologies this number is just increasing. The creation of transmission corridors in natural habitats can have an effect on biodiversity similar to the PV power plant itself. In short term the corridors are used by new communities to reach new territories and it can be an issue. However in a mid-late term some places have presented great side effects on native biodiversity. In conclusion the environmental effects of the transmission lines are strongly correlated with the location and can be mitigated.

According to [10] the spanish transmission system in 2016 had 43.800km of circuits and 5.609 substation bays accounting a total power of 85.144 MVA. The tendency is to grow with values between 0 and 1%. As a example in the 2018 review of *Red Eléctrica de España* ([12]) the total length of the transmission system is 44.243km.

In high capacity transmission systems the losses can affect directly to the climate change. In average the losses represent up to 3% of the total energy flow. This can represent a high volume of energy flowing to the environment leading to local temperature changes.

A lot of components used to conform the transmission lines and the interaction elements of the grids, such as oil from transformers, contain environmental harassing substances that shall be recycled properly in order to mitigate their negative effects.

5.1.7 Conclusions

In general, positive impacts outweigh negative ones. At first sight the relief of the conventional generation plants in favour of solar energies is a good deal due to the reduction in CO_2 and gas emissions. However many things need to be taken account to mitigate the possible side effects of solar energies. For example if a LS-PVPP is located in a environmentally sensitive ecosystem the biodiversity would be strongly affected. In conclusion a

ETSEIB

deep study on the location, a mitigation plan and a correct law code that protects the more sensitive areas can conclude in many environmental and social benefits.

Chapter 6

Projects budget

The present work is centered in the optimization of a PV plant by including a tool that allows the user to take advantage of real time information to reduce losses and choose the best settings at each situation. The cost of implementation is relatively low in comparison to the total budget of creating an entire PV power plant and it can have positive economic effects as consequences. Different conception costs per energy unit are presented. In first place the CAPEX[I] (capital expenditure, table 6.1) data for a LS-PVPP project are presented. In second place OPEX[II] (Operational expenditures, table 6.2) derived from the continuous operation of the PV plant are tabulated. Finally a small review of the economic impact of the ancillary services is presented according to *Red Eléctrica de España*.

6.1   Large Scale PV power plant

The prices shown on table 6.1 are extracted from [2]. The data is extracted from Bloomberg New Energy Finance which is a reliable energy related database. The battery system commented in section 4 is included to illustrate the high cost per kWh of this methodology. The miscellaneous cost include an average land prince and the engineering, the derived cost of legal permissions and the construction among others.

Where EUR/W_n is the cost per watt of nominal power. The Balance of the system (BOS) encompasses all the components of a photovoltaic system other than photovoltaic panels and the inverters. This concept includes wiring, switches, mounting system and some mechanism used to increase the efficiency of the PV power plant such as the maximum power point tracker (MPPT) or the GPS solar tracker that changes the orientation of the panels depending on the position of the Sun.

In the table 6.2 the continuous operations cost for a year of production is presented. The PV technologies need energy to start converting energy and the intermittency of the solar

---

[I]CAPEX; the inversion cost to start running the PV plant.
[II]OPEX; the operation and maintenance cost of running the PV plant.

Table 6.1: PV plant CAPEX costs and current project budget

CAPEX component	Cost per Watt	Current project
Modules	0,31 EUR/W_n	1,24 M. EUR
Central inverters	0,03 EUR/W_{AC}	0,12 M. EUR
Balance of the system	0,17 EUR/W_{AC}	0,68 M. EUR
Miscellaneous cost	0,30 EUR/W_{AC}	1,2 M. EUR
Power curtailment with batteries (optional)	400 EUR/kWh	-

source or the night periods create situations where the consumed energy is higher than the production. The dust removal, panel cleaning, maintenance products and salaries are included. The tracker system operation cost is isolated to illustrate the associated cost of implementing a solar tracking system.

Table 6.2: PV plant OPEX

OPEX component	Cost per MW
OPEX PV plant operation	9500 EUR/MW
OPEX tracker operation (if included)	900 EUR/MW

6.2   Ancillary services

The grid codes requirements have an impact on the average final price of energy. In the report of *Red Eléctrica de España* of 2018 about the ancillary services [11] a breakdown of the components conforming that price is performed. The figure 6.1 illustrates it. The grid support requirements seen in section 4 introduce a reduction on the final price. The magnitude of its reduction is small in comparison with the final price but the advantages in energy management in terms of reliability and security make their application essential.

ETSEIB

Price [€/MWh] [1]	Aug	Sep	Oct	Nov	Dec	Total
Day-ahead market	65.00	71.78	66.10	62.94	62.63	58.12
Intraday market	-0.05	-0.01	-0.04	-0.04	-0.05	-0.03
Ancillary Services	2.99	2.27	1.93	1.18	1.28	2.35
Technical constraints PDBF[2]	1.75	1.10	0.94	0.67	0.77	1.47
Additional upward power reserve	0.72	0.64	0.31	0.08	0.11	0.23
Secondary control band	0.47	0.49	0.63	0.41	0.34	0.55
Real-time technical constraints	0.04	0.02	0.04	0.02	0.06	0.07
Non-fulfilment of balancing energy	-0.02	-0.03	-0.03	-0.03	-0.04	-0.03
Deviation cost	0.12	0.10	0.09	0.08	0.11	0.15
Deviation balance	-0.04	-0.03	0.03	0.02	0.00	-0.04
Power factor control	-0.04	-0.04	-0.06	-0.06	-0.06	-0.06
Operating Procedure 14.6 balance	-0.01	0.02	-0.02	-0.01	-0.01	0.01
Capacity payments	2.16	2.41	2.40	2.56	3.14	2.71
Interruptibility service	1.03	1.10	1.13	1.10	1.08	1.23
Average final price 2018	71.13	77.55	71.52	67.74	68.08	64.38
Average final price 2017	54.69	56.28	64.83	66.81	67.32	60.55
Final energy [3] [GWh]	21,946	20,697	20,270	20,878	21,137	253,174

[1] Prices are calculated using the latest settlements available from the System Operator.

[2] PDBF: Daily Base Operating Schedule.

[3] Includes closing of the energy market and own consumption of power generation ancillary services.

Figure 6.1: Breakdown of ancillary services cost in the average final price of energy in the peninsular system

ETSEIB

Conclusions and further work

During the last years solar energy has penetrated in the energy market as an alternative to fossil fuel-based energy. It has been possible due to the advances in power electronics mixed with the automatic control methodologies that permitted the mitigation of the unintended behaviour of renewable energies. The balance of the environmental effects brought by these renewable energies is mostly positive however in section 5 is shown that the effects on the environment are diverse and strongly dependent on the situation and the ecosystem sensibility. In some cases those consequences are unknown and can conclude in a permanent change in the surroundings of the installation with important losses in biodiversity and natural wealth. In consequence a deep study on the biodiversity and present ecosystem shall be performed in order to mitigate those negative effects. The soil and physic environment are also affected as a part of the energy they were usually receiving to develop natural processes is used to produce energy for human consumption causing changes in the local temperature and soil nutrients development.

In the current work a program based on [3] to solve the power flows of a given system is developed and validated versus MATPOWER. It models the buses using traditional methods as PQ and PV buses. A summary of the most common static regulation present in most of the grid codes is included. A particular solution to mitigate the negative effects of the unintended reactive power on large distribution systems based on regulating the amount of reactive power as a function of the voltage is also included. In further work the implementation of that bus model and more grid code requirements can be performed.

Although the good results achieved by energy storage systems and the new developments the implementation cost is still high in order to be competitive. Thus, the active power reserves methodology discussed in section 4.2.3 leads to a efficiency decrease.

Annex

6.3 Introduction

In this chapter different images and script information from this work can be found.

6.4 Scripts

A brief description of the scripts used in the present project is included next. The scripts can be found in the .zip file annexed to this project.

- The scripts named *busdatas* and *linedatas* are extracted from [3] and are used to introduce each case initial data. The information about the data introduction is discussed in section 3.2.2.

- *ymatrix* is used to create the admittance matrix.

- *pfeq* and *pfeq2* are the core of the NRA. Their results are the voltage and phase values of the buses. The difference between them is the way of displaying the results.

- *loadflows1* and *loadflows2* are used to perform the load flow analysis. They are called from *pfeq* and *pfeq2* respectively.

- The *Surface* script is used to validate the results against MATPOWER and identify particular points if needed. It varies two parameters of the system and plot the results in different surfaces for both programs. The different parameters that can be changed are: active and reactive power demand (P_l, Q_l), active and reactive power generation (P_g, Q_g), all converters voltage at the same rate (only PV buses; V_{11}, V_{12}, V_{13} and V_{14}) and the grid voltage (V_1).

- The *linear* script is made for a two dimension comparison to study the behaviour in a more isolated manner than in the *Surface* script.

- The *linear pfe* script perform simulations of changing one parameter and plots the results in two dimension graphics. The available parameters to change are the same from *surface* script.

- The *individual case* script perform one simulation of the selected case and displays an accurate summary of the values of the system. A breakdown of the branches and buses values as well as the totals are included. In addition in cases including PV buses the limit violations are also displayed.

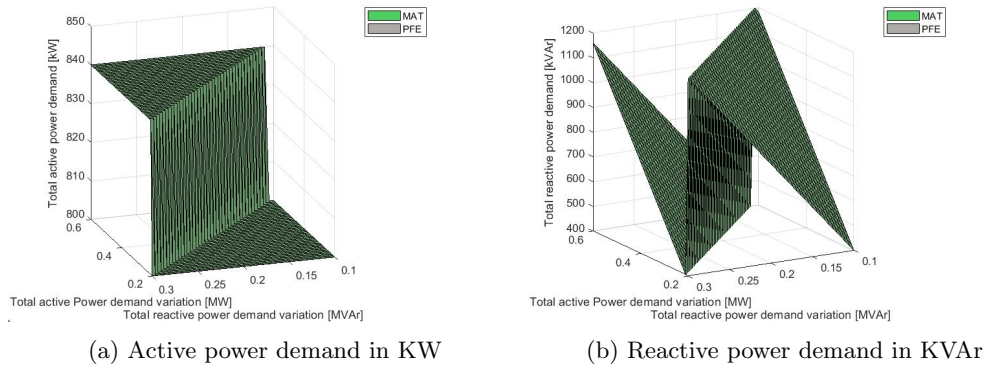## 6.5 First comparison power flow results

(a) Active power demand in KW

(b) Reactive power demand in KVAr

Figure 6.2: Active and reactive power demand (1st case)

(a) Active power generation in KW
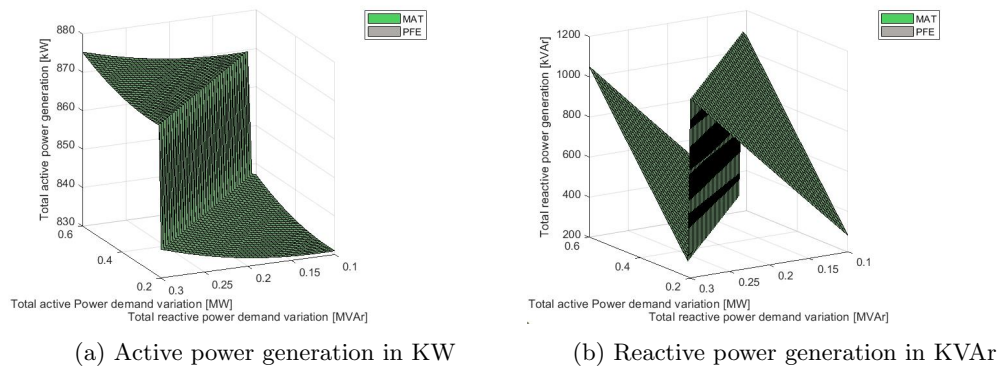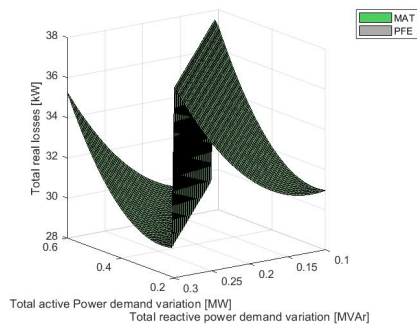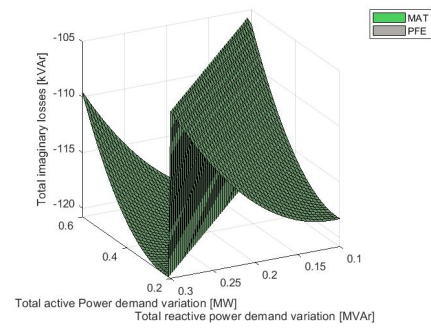
(b) Reactive power generation in KVAr

Figure 6.3: Active and reactive power generation (1st case)

(a) Real losses in KW

(b) Imaginary losses in kVAr

Figure 6.4: Imaginary and real losses (1st case)
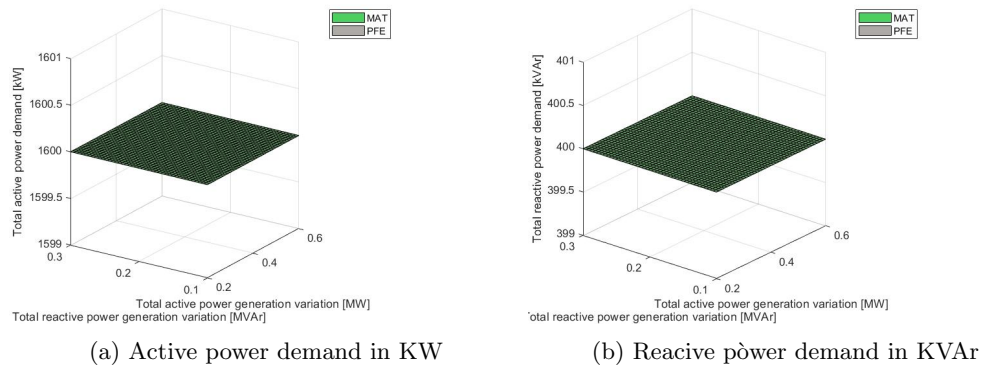
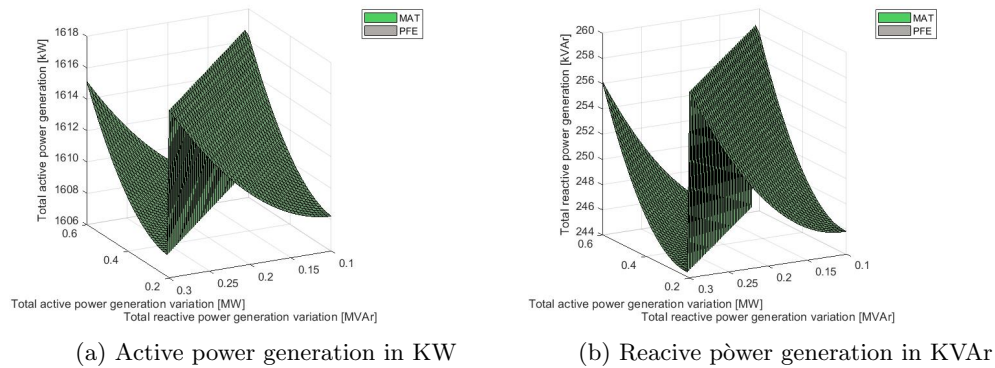## 6.6   Second comparison power flow results

(a) Active power demand in KW

(b) Reacive pòwer demand in KVAr

Figure 6.5: Active and reactive power demand (2nd case)

(a) Active power generation in KW

(b) Reacive pòwer generation in KVAr

Figure 6.6: Active and reactive power generation (2nd case)
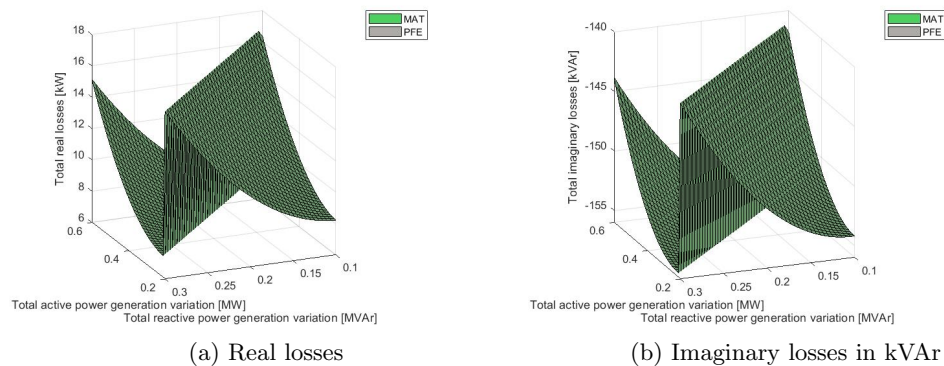

(a) Real losses

(b) Imaginary losses in kVAr

Figure 6.7: Active and reactive power generation (2nd case)

6.7 Third comparison power flow results

(a) Active power demand in KW

(b) Reactive power demand in KVAr
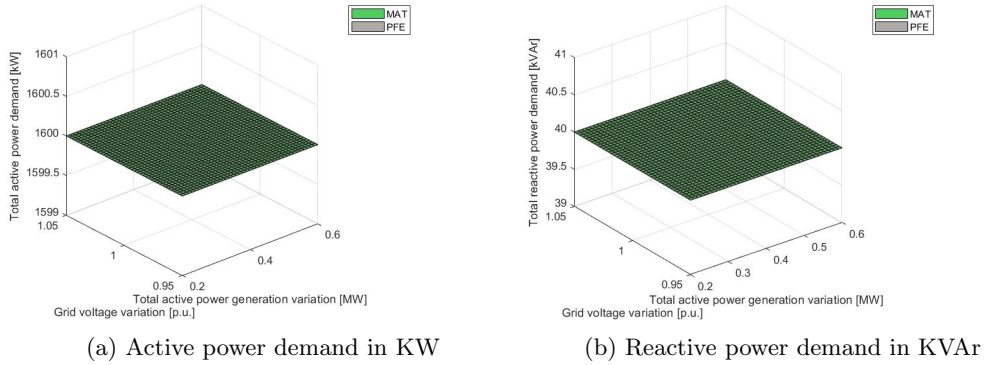
Figure 6.8: Active and reactive power demand (3rd case)

(a) Active power generation in KW

(b) Reactive power generation in KVAr
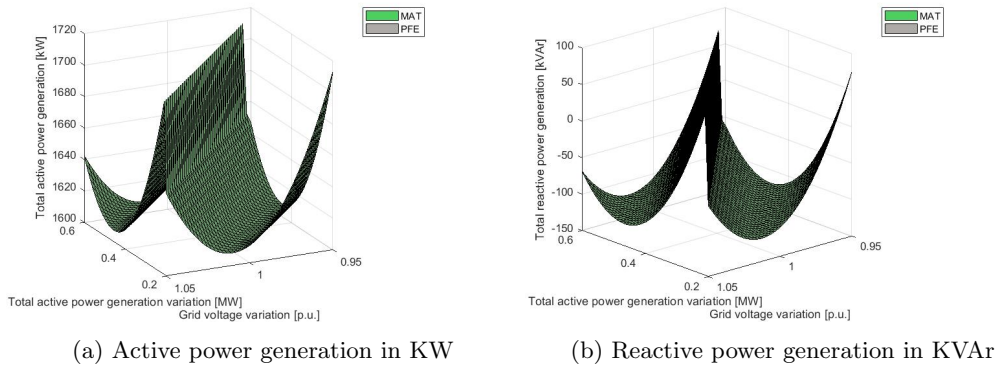
Figure 6.9: Active and reactive power generation (3rd case)

(a) Real losses

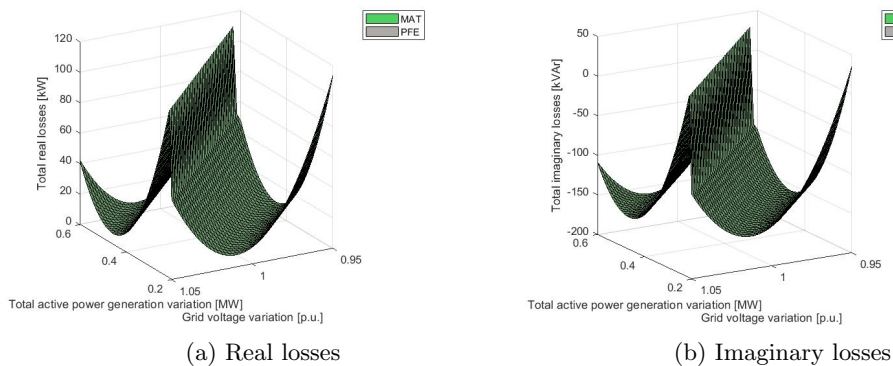(b) Imaginary losses

Figure 6.10: Active and reactive power generation (3rd case)

Bibliography

[1] Gabriele Catalano, Oriol Gomis Bellmunt. *Development of a model to simulate solar PV plants in MATLAB with a study on the effects of undersizing the inverter* Master thesis from ETSEIB, UPC. September 2018.

[2] Eduard Foved Johe, Oriol Gomis Bellmunt. *Design and optimisation of the architecture and the orientation of utility-scale photovoltaic power plants* Master thesis from ETSEIB, UPC. April 2019.

[3] Praviraj PG (2020). *Newton-Raphson Loadflow*(https://www.mathworks.com/matlabcentral/fileexchange/21059-newton-raphson-loadflow) , MATLAB Central File Exchange. Retrieved May 24, 2020.

[4] Willi Christiansen and David T. Jonhsen *Analysis of requirements in selected Grid Codes* Ørsted•DTU, Section of Electric power Engineering, Technical University of Denmark (DTU). 20 January 2006.

[5] Ana Cabrera-Tobar, Eduard Bullich-Massagué, Mònica Aragüés-Peñalba and Oriol Gomis-Bellmunt. *Active and Reactive Power Control of a PV Generator for Grid Code Compliance* Energies. 12. 3872. 10.3390/en12203872.

[6] Raquel Fernández-González, Andrés Suárez-García, Miguel Ángel Álvarez Feijoo,Elena Arce and Montserrat Díez-Mediavilla. *Spanish Photovoltaic Solar Energy: Institutional Change, Financial Effects, and the Business Sector* (www.mdpi.com/journal/sustainability) Sustainability 2020, 12, 1892; doi:10.3390/su12051892

[7] Atsede G. Endegnanew, Salvatore D'Arco, Atsede G. Endegnanew, Raymundo E. Torres-Olguin, Jorun Irene Marvik and Elisabetta Tedeschi. *Collocation of European grid codes* Work Package Partners, doc ref: MARINET-D2.26.

[8] Henrik Alenius, Roni Luhtala, Tuomas Messo, Tomi Roinila. *Autonomous reactive power support for smart photovoltaic inverter based on real-time grid-impedance measurements of a weak grid* doc ref: https://doi.org/10.1016/j.epsr.2020.106207. 2020 May.

[9] R.R. Hernandez, S.B.Easter, M.L.Murphy-Mariscal, F.T.Maestre, M.Tavassoli, E.B. Allen, C.W.Barrows, J.Belnap, R.Ochoa-Hueso, S.Ravi, M.F.Allen. *Environmental impacts of utility-scale solar energy* Renewable and Sustainable Energy Reviews Volume 29, January 2014, Pages 766-779. https://doi.org/10.1016/j.rser.2013.08.041

[10] Red Eléctrica de España *The Spanish Electricity System 2016* ONLINE: Review of the Spanish electricity system from 2016.

[11] Red Eléctrica de España *Ancillary services and International exchanges ONLINE: PRELIMINARY REPORT: Commited to Intelligent Energy 2018*

[12] Red Eléctrica de España *Red Eléctrica Infografia Sector Electrico* ONLINE Poster 2018